January 2001

Single Cone Mirror Omni-Directional Stereo

Shih-Schon Lin
University of Pennsylvania, shschon@seas.upenn.edu

Ruzena Bajcsy
University of Pennsylvania

University of Pennsylvania Department of Computer and Information Science Technical Report No. MS-CIS-01-03.

Single Cone Mirror Omni-Directional Stereo

Abstract

Omni-directional view and stereo information for scene points are both crucial in many computer vision applications. In some demanding applications like autonomous robots, we need to acquire both in real-time without sacrificing too much image resolution. This work describes a novel method to meet all the stringent demands with relatively simple setup and off-the-shelf equipments. Only one simple reflective surface and two regular (perspective) camera views are needed. First we describe the novel stereo method. Then we discuss some variations in practical implementation and their respective tradeoffs.

Comments

University of Pennsylvania Department of Computer and Information Science Technical Report No. MS-CIS-01-03.

Single Cone Mirror Omni-Directional Stereo

Shih-Schön Lin, Ruzena Bajcsy
Technical Report MS-CIS-01-03
GRASP Laboratory, Computer and Information Science Department
University of Pennsylvania,
shschon@grasp.cis.upenn.edu , rbajcsy@nsf.gov (also, bajcsy@grasp.cis.upenn.edu)

Abstract

Omni-directional view and stereo information for scene points are both crucial in many computer vision applications. In some demanding applications like autonomous robots, we need to acquire both in real-time without sacrificing too much image resolution. This work describes a novel method to meet all the stringent demands with relatively simple setup and off-the-shelf equipments. Only one simple reflective surface and two regular (perspective) camera views are needed. First we describe the novel stereo method. Then we discuss some variations in practical implementation and their respective tradeoffs.

1. Introduction

Autonomous robot vehicles need to survey the entire environment around it constantly in real-time in order to avoid obstacles and perform more advanced functions like scouting, exploration, target detection and tracking...etc. It is also important to do the detection passively in many situations to conserve power and remain stealthy.

The most widely used passive ranging is stereo rigs composed of two perspective cameras. Since most perspective cameras have limited Field Of View(FOV), one can get stereo range in only one direction at a time. Many researchers have added rotational device to rotate cameras to get the whole omni-directional view, for example Sarachik [B16], Ishiguro *et al.*[B7;B8], Murray [B13], Kang and Szeliski [B9]. Krishnan and Ahuja [B11] rotate their special NICAM, a tilted image plane camera, to get panoramic depth from focus. To get even higher resolution some setup rotate one or two line scan cameras instead of ordinary cameras, e.g. Benosman *et al.* [B2]. These methods produce very high resolution omni-directional stereo data for static scenes. But since they need mechanical scanning they can not acquire data in real time and fast moving objects in the scene may disrupt the correspondence matching algorithms.

To avoid the time-consuming scanning some setups use a lot of fixed cameras, like the system from Nara, Japan [B10]. Such systems achieve high resolution omni-directional stereo with very high costs. The system from Nara, for example, uses 12 cameras and 12 mirrors. The setup itself is expensive and hard to miniaturize. In addition, the high volume of data flow created by so many cameras recording live video simultaneously puts a lot of demand on data storage and processing. Thus while real time stereo information can be recorded, the stereo information must be extracted off-line in practice. The calibration and synchronization problems are also fairly complicated for a system with so many cameras.

Recently catadioptric omnidirectional system is gaining popularity over both the scanning method and multi-camera method mentioned above because of system simplicity. No mechanical rotation is needed and at most two fixed cameras are needed in the new catadioptric systems. Real-time is feasible because all scenes are taken simultaneously and the image data to be processed is much less than those required by multi-camera setups. Using only one camera, Nayar [B14], Bogner [B3], Southwell *et al.* [B17] and Nene and Nayar [B15] can get omni-directional stereo in real-time and avoid many nasty calibration problems altogether. The trade-off, however, is the relatively low image and range resolution, plus limited depth accuracy due to short base line confined by camera FOV. Using 2 cameras, Gluckman *et al.*[B5] double the resolutions while retaining most of the advantages of catadioptric omni-systems. The system, however, requires two complex mirrors and two special lens sets(orthographic lenses).

The system proposed in this work uses only one simple convex mirror and two views from ordinary perspective cameras. The resolutions are five to ten times better in typical usage than the two curved omni-mirror setup and the stereo computation is simpler and faster. In addition, the FOV of one view is completely contained in the other so the loss of correspondence due to different viewing direction in two views is greatly reduced.

2. Real-time Omni-Directional Stereo System with High Resolution

Figure 1 is a diagram of the basic concept of our system. A cone shape mirror at the top forms a perfect virtual image point behind the mirror surface for each world point within the FOV of the cone mirror. This is done entirely by the mirror itself, with nothing to do with any other cameras. So for the two perspective camera views, the 3D position of any virtual image point is the same. The 2D image position of the same 3D point will be different with different viewpoint and focal length, and the 2D position change is directly related to the depth of the 3D point. Thus, after correspondences of image points in the two views are established, the depth can be recovered.

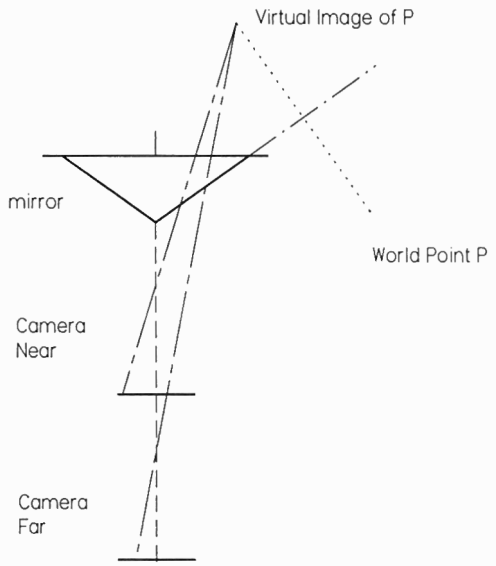

Figure 1 Conceptual overview of the omni-stereo system

The two views are completely aligned with the axis of symmetry of the cone mirror. This arrangement yields 3 major advantages: First, the epipolar geometry is automatically taken care of. Correspondence always occurs at the same radial line from the center of the cone. Second, the dynamic range of the depth is much greater than the traditional 'side by side' stereo setup, i.e. the line of sight of the two views are not the same line. Third, the FOV of the near view is always completely contained in the far view. This basically ensures that every image point in the near view will have a match on the far view. This is not the case for traditional "left an right view" stereo. In actual systems, the near camera can be physically placed away from the center of symmetry by the use of a beam splitter yet remain effectively aligned with the far camera.

2.1 Recovery of Virtual Image Positions

Depth recovery of our "near and far" coaxial arrangement is illustrated in Figure 2. Here depth z is measured from the near camera projection center. The stereo baseline b is the separation between the near camera and far camera projection centers. The near camera and far camera has focal length f and f' respectively. The image positions of the same point P in the near and far view are x and x' unit away from the image center respectively.

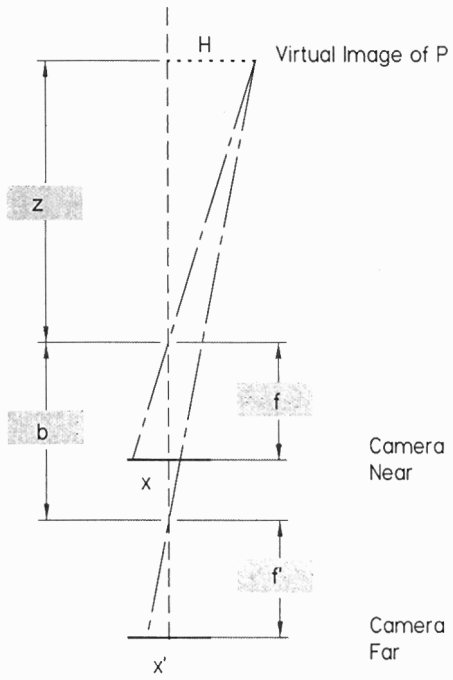

Figure 2 Virtual depth recovery geometry

From similar triangles we have the following:

$$\begin{cases} \dfrac{x}{f} = \dfrac{H}{z} \\ \dfrac{x'}{f'} = \dfrac{H}{z+b} \end{cases}$$

Equation 1

divide and simplify, we get

$$z = \frac{b}{\left(\dfrac{x}{x'}\right)\left(\dfrac{f'}{f}\right) - 1}$$

Equation 2

In most cases where f=f', we have

$$z = \frac{b}{\frac{x}{x'} - 1}$$

Equation 3

2.2 Recovery of Real 3D Depth

Once the exact position of a virtual image point relative to the camera is known, we can derive the positions of the real world points because the geometry of the setup is known.

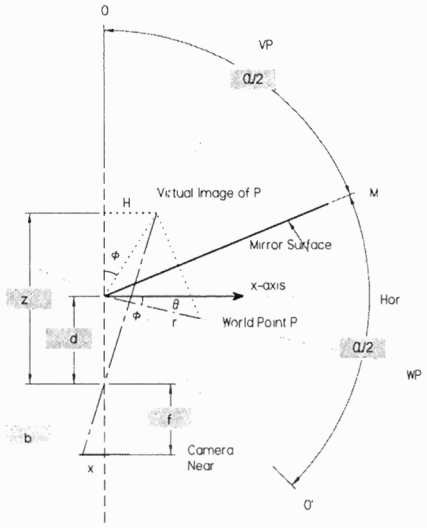

Figure 3 Relationship between the real depth r and the virtual image point depth z

In order to recover the 3D position of a world point P, we need to recover 3 quantities: the azimuth angle, the elevation angle, and the distance r to the origin of the coordinate system. Here we put the origin of the spherical coordinate system at the tip of the cone mirror, where its intrinsic single view point is located (see [B1;B12]).

The system can always be set up such that the azimuth value directly corresponds to the azimuth angle of its image point, so only the remaining two coordinates need to be computed. Figure 3 depicts the 2D vertical cross section of our system. We want to compute r and θ given all other values. The quantities in Figure 3 have the same meaning as their counterparts in Figure 2. In addition, d is the distance of the near viewpoint to the tip of the cone. The cone mirror subtends an angle α at its tip and φ is the angle of the virtual image point from the vertical axis relative to the tip of the cone. The elevation angle θ here is zero at the horizon(x-axis) and increases downward. First we have

$$\tan\phi = \frac{H}{z-d} = \left(\frac{z}{z-d}\right)\left(\frac{x}{f}\right)$$

Equation 4

From the properties of plane mirror reflection, we derive the relationship between φ, α and θ as

$$\theta = \alpha - \phi - \frac{\pi}{2}$$

Equation 5

The constant π/2 shows up because we choose the horizon to be the direction that corresponds to θ=0. In Figure 3, θ is the angle between directions WP(World Point) and Hor(Horizon). θ is positive when the direction WP is below the horizon. φ is the angle between the direction VP(Virtual Image Point) and the direction O(the optical axis of the near and far cameras) relative to the tip of the cone. The angle between O and M(Mirror surface to the right) is α/2. Since O and O' are mirror image of each other and WP and VP are mirror image of each other, the angle between O and O' is α, and the angle between O and WP is α-φ. As θ is measured between Hor and WP, we subtract the angle from O to Hor (always π/2) from the angle between O and WP and we have Equation 3. Since mirroring operation preserves distances, the real world depth r is the same length as its mirror image counter part, which is

$$r = (z-d)\times\sec\phi = \frac{\sqrt{z^2x^2 + (z-d)^2 f^2}}{f}$$

Equation 6

2.3 Field of View

To assist the explanation of our usable FOV, we use the concept of *virtual camera*. Simply put, in terms of plane mirrors, the image formed with a real camera looking at the virtual world behind the mirror surface is exactly the same as the image formed with the virtual camera behind the mirror surface looking at the real world scene outside the mirror. This is a direct result of the symmetry of the physical formula involved in optical image formation, see optics text like Hecht [B6] for details. Gluckman and Nayar also used this virtual image concept extensively [B4].

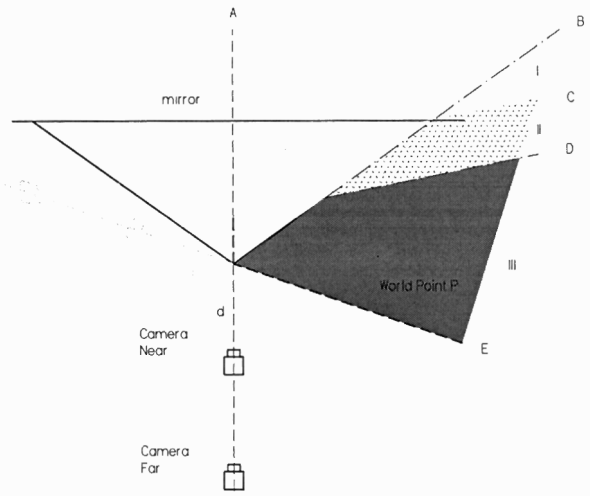

Figure 4 Vertical FOV usable for stereo

The position of the virtual camera is just the virtual image of the real camera created by the plane mirror that reflects the light rays producing the image. The vertical cross section of the cone mirror used in our system is exactly the same as that of two plane mirrors and in the vertical direction acts exactly like plane mirrors. The FOV of the two sides are symmetric so we show in Figure 4 only one side to avoid cluttering the figure with too many overlapping lines.

In Figure 4 the two real cameras have their corresponding 'virtual cameras' on the upper left, shown in light gray. The 'virtual camera' of the near camera is still closer to the tip of the cone. The letter A~E represents straight lines that divide the space into zones I~III.

- A: the axis of symmetry of our system
- B: the extension of the right mirror surface
- C: the FOV limit of virtual far camera
- D: the FOV limit of virtual near camra
- E: the lower FOV limit of every FOV considered here. In fact this is the mirror image of line A with respect to right mirror surface.

The cone itself has the largest FOV, including zone I, II and III, or the space between line B and line E. Every world point within this zone has a virtual image inside the right side of the cone. If the cone tip angle is α, the angle between line A and line E is α, too.

Zone II, the zone between line C and D and to the right of B is the area visible by the virtual far camera and the cone. Zone III, the area between line D and E and to the right of line B, is the area visible by all devices. Only the area visible by all is usable for stereo, so the useful FOV for our system is the area filled with solid gray. When the FOV of far and near view are the same or the far FOV is bigger than near FOV, anything seen by near view is guaranteed to be visible in the far view.

It is worth mentioning the changing the FOV of near and far camera changes line C and D only, as the points on the direction of line E is always imaged to the image center of the two omni-view images. Scene points on the direction of line C and D are imaged to the edge of far and near omni-view image respectively. Line E is the mirror image of line A so can only change direction by changing the angle of the cone.

2.4 Epipolar Constraint

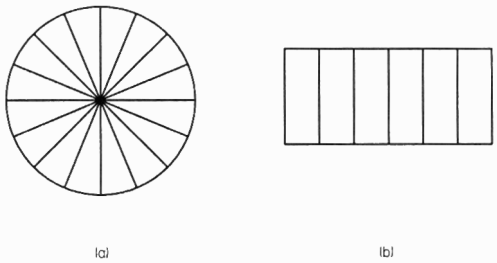

Figure 5 Epipolar geometry. (a) omni-view (b) panorama view

One of the major advantage of our setup is the simple epipolar geometry. For omni-views the epipolar lines are radial lines. For panorama view the epipolar lines are vertical parallel lines. Exact panorama can be synthesized after the virtual depth (z) values are determined. For finding correspondence purposes, non-exact panorama is not a problem as we shall explain later.

3. System Performances

3.1 Image Resolution

Image resolution is the number of pixels used to see a sector of the scene. For methods using one or two views to capture stereo, especially for real-time stereo, the whole scene around it is crammed into one TV resolution image.

In our method and [B17;B5], the maximum azimuth resolution are all the same, about $480*\pi/360$ degree, that amounts to about 4 pixels per degree. The resolution degrades toward the center of omni-view until it is 0 pixels right at the center. In comparison, with traditional optics with 40 degree FOV, the resolution is 640/40=16 pixels per degree. On average the azimuth resolution is only 1/8 of normal. This is an unavoidable tradeoff of speed, price and quality that is common to all the omni-view devices using only one or two images to capture all the scenes.

For vertical resolution, our method is as good as the conventional cameras because vertically they see the same

angle per pixel. For methods using mirrors that are curved vertically, like parabolic and hyperbolic mirrors, their vertical resolution is non-uniform but on average 5 to 10 times worse because their vertical FOV is 5 to 10 times larger while the number of pixels available remains the same. Using the same CCD chip, traditional optics typically have FOV from 20 to 40 degree while for vertically curved omni-mirrors their FOV is 180 degrees or larger.

For methods using one view to look at two convex mirrors, the resolution is basically halved. With carefule arrangement such system can improve a little resolution but is less than 2/3 of our system.

3.2 Depth Resolution

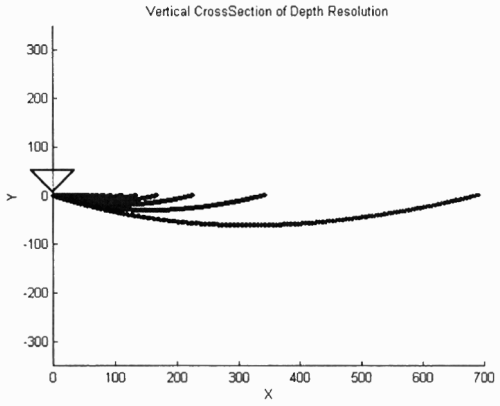

Figure 6 Depth resolution. Each point represents the 3D position corresponding to a pair of correspondence. The system parameters of this graph are b=2, d=3, lens camera FOV 23 degree, cone tip angle 113 degree, image resolution is 320 pixels along one epipolar line. The origin of coordinate is located at the tip of the cone mirror. The cone mirror drawn here is NOT to scale.

The depth resolution is non uniform across the omni-view image. Depth depends not only on the position differences in the two views, but also on the position of the image point. Combining Equation 2 and Equation 6 we have the rather complicated expression of real depth. The meaning of which is best visualized by plotting the world point positions for all possible pixel correspondence pairs x and x' in a vertical cross section view, see Figure 6 and Figure 7.

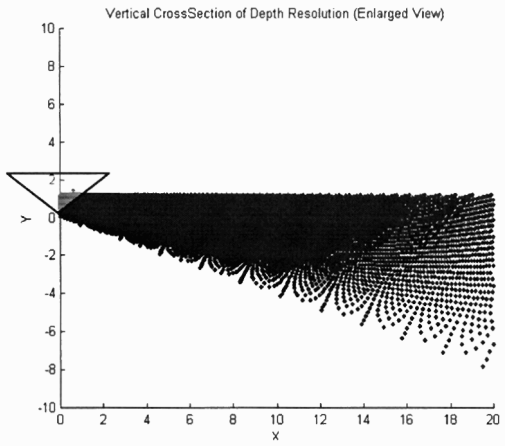

Figure 7 Enlarged View of Depth Resolution, the cone mirror drawn here is NOT to scale, just to help visualization.

Note that both Figure 6 and Figure 7 are dot plots only, no lines connect any two dots. The dots are so dense that they seem to form connected lines. This means the system has good depth resolution as fine details of depth information can be resolved.

In Figure 6 we see that for far away scenes, dot density is low which means poor depth resolution. Figure 7 is a zoom-in view around the origin (the tip of the cone). It shows clearly that closer scenes have good depth resolution as points are dense and more uniformly distributed. As a rule of thumb, scenes within 100 times the baseline have good depth resolution.

3.3 Depth Dynamic Range

Although the general depth formula are quite complicated, in practice we can often simplify the formula because d is usually very small compared to z and often we prefer to make f=f'. The simplified formula are:

$$\begin{cases} \tan\theta = \dfrac{x}{f} \\ r = z\sec\theta = \dfrac{b}{\dfrac{x}{x'} - 1} \times \dfrac{\sqrt{x^2 + f^2}}{f} \end{cases}$$

Equation 7

Typically d is of the order of a few centimeters, while z is of the order of tens of meters, so the simplification is pretty justifiable. In Equation 7 the depth is scaled by baseline b, typical of triangulation based stereo. The maximum possible depth is infinity. But due to

digitization the maximum distinguishable depth for a given x is when x'=x-1. Beyond this range any object will have disparity less than one pixel. When x'=x-1, z=x'b, so the usable dynamic range is greater when there are more pixels in the camera we use.

The minimum possible depth is 0, when x'=0. In practice we seldom use omni-directional device to look at scenes so close to the mirror.

3.4 Bonus Single View Point unwarping

Because our system extracts exact 3D positions for each scene point, we can synthesize perspective views from any viewpoint. Including the single viewpoint view from the cone mirror tip. The BRDF effects are minimal in most cases because the near camera is not far from the true single viewpoint. Thus besides recovering omni-directional depth information, we recover a single view point omni-directional view as well, using a setup that is not physically single viewpoint by itself.

4. Experiments

Our prototype system consists of a chrome-plated aluminum cone as the cone mirror, a SONY XC-003 3CCD with Canon JF25mm 1:1.4 TV Lens as our perspective camera, a BIG JACK lifting platform by GCA\Precision Scientific to move the camera up and down. In a commercialized version more compact design using beam splitter cube is possible. Our prototype is used only as a proof of concept so everything is done in the cheapest way. The alignment of optical axes is done by using gravitational horizon as the reference. After the camera is looking straight down we move the cone mirror horizontally, until the tip of the cone is imaged approximately at the image center. Fine adjustment of image center is done later by digital shifting (typically within 5 pixels). We also assume the lifting platform introduces no horizontal shifting when lifting the camera up and down. We get intrinsic camera parameters using the specifications provided by the manufacturers and adjust the focal length using thin-lens formula and focusing information.

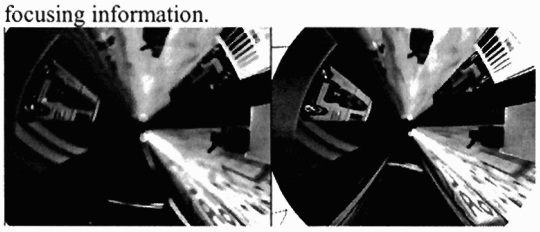

Figure 8 Two omni-views for experiment. The viewpoint of the left image is 10.3 inch while the right image is 12.3 inch above the tip of the cone mirror.

Figure 9 Top: Rectified image of high view. Bottom: Rectified image of low view.

Figure 10 Panoramic gray coded range map from the SVP of the cone mirror.

We used 3 CCD color camera in order to exploit color texture information. The omni-views taken from the camera are shown in Figure 8. The rectified images are shown in Figure 9. The panoramic gray coded range image obtained by standard normalized correlation (15 by 3 window) is shown in Figure 10. The range values of area with no good correspondence due to lack of texture are set to zero. The results shows that wherever good correspondence is found, range data can be reliably extracted.

5. Simulations

The purpose of simulation is to demonstrate the system performance under ideal conditions. Imperfections in optics, axis alignments, frame grabber, ...etc can be avoided. We use a 3D ray tracing graphics package called POV-ray to generate a world consisting of 4 walls, some vehicles, trees and a building. Each of which is covered with texture to assist in automatic correspondence matching. Note that this "synthetic scene" is much more complex than "random dots synthetic stereo images". The ray tracing program models shading and lighting condition changes just like in the real images. So the results we get is very close to what we will get with real images.

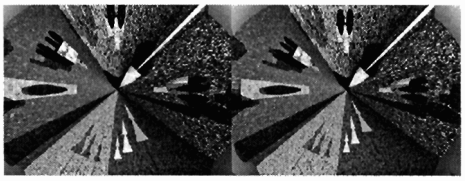

Figure 11 Two omni-views for simulated world. The left image is at the SVP. The right image is taken 3 unit higher.

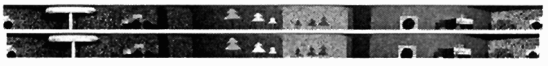

Figure 12 Top: Rectified image of high view. Bottom: Rectified image of low view

Figure 13 The panoramic gray coded range map from the SVP of the cone.

Figure 14 Using only range information, vehicles, trees and buildings can be extracted.

The two views are 3 units apart vertically and has the same focal length (vertical FOV 34 degree). The cone mirror simulated here has top angle 107 degree. The generated image is the standard NTSC resolution 640x480 pixels. We generate the rectified images with 5082x240 pixels (this preserves aspect ratios for single view point view and prevent aliasing caused by undersampling). The two omni-view images are shown in Figure 11.The rectified images are shown in Figure 12. The correspondences are found by standard window-based (15 pix vertical by 1 pix horizontal) normalized correlation measure. The resulting gray-coded panoramic range image is shown in Figure 13. Also we can segment out the vehicles, the building and 2 trees using only the range information, as shown in Figure 14. This result demonstrates the viability of our omni-directional range recovery system.

6. Discussions

As proved by Baker and Nayar [B1], when the viewpoint of a perspective camera coincides with the tip of a cone mirror, you have a single viewpoint omni-view system. Lin and Bajcsy went a step further to prove that this single viewpoint is actually usable. The new system proposed here consists of one cone shape mirror surface with two perspective views taken directly above the cone mirror. The optical axis of both views are aligned with the central axis of the cone mirror. Such configuration has two major advantages. First, the FOV of the far view always cover the entire FOV of the near view, which means that every scene point of the near view image will be visible in the far view. This is not the case for many stereo systems. Another good feature is the simplicity of the important epipolar geometry. Gluckman *et al.* [B5] proposed a system with the same simple epipolar geometry. As pointed out the Gluckman *et al.* the simple epipolar geometry saves time and improves accuracy of correspondence matching.

When we directly align two real cameras in a tandem configuration, the near camera may block all or part of the view of the far camera. The most direct solution is to place a beam splitter to split the views. When the mirror is larger than the near camera, one can simply live with a smaller system FOV. As digital cameras are made smaller and smaller the occlusion zone can become small enough for small mirrors to work without a beam splitter.

There is an inevitable tradeoff in all the omni-directional vision devices that uses only one image to capture the whole omni-view. That is the relatively low resolution. In azimuth direction there is not much to be improved except using higher resolution imaging device. For example, Nene and Nayar [B15] used normal TV standard CCD to capture images for non-omni-directional stereo, but need to use conventional 35mm SLR camera with films plus high resolution scanner for the omni-directional stereo.

Our stereo device presents a better tradeoff in terms of resolution. Compared to methods looking at two omni-mirrors with one single picture, our resolution is roughly twice as good because the same number of pixels is concentrated on one mirror only. Gluckman's system [B5] also looks at one mirror per picture, but our system has higher vertical resolution than they do. The tradeoff here is that our vertical FOV is smaller, but in many applications this means we concentrate the limited number of pixels on the most interesting area. The extra FOV they have is around the direct downward direction and when the stereo device is mounted on a vehicle these area are usually blocked anyway, see Figure 15. By concentrating available pixels on the useful view angle, each scene feature is covered by 5~10 times more pixels and results in better image resolution, better depth resolution, and better correspondence accuracy.

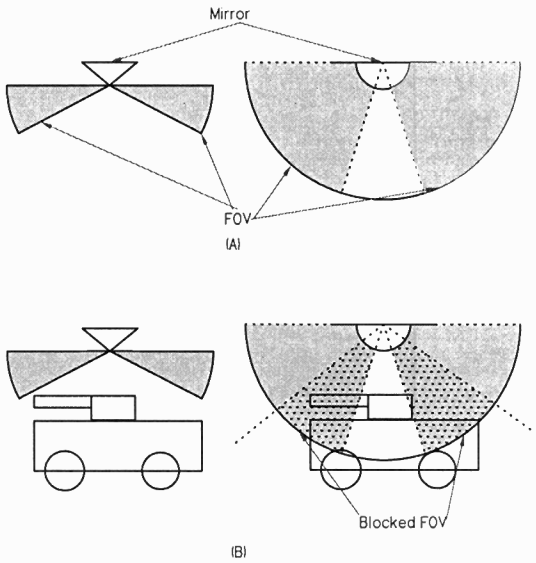

Figure 15 FOV comparison of vertically flat and curved mirrors

The FOV of our system is also more flexible because we can change the vertical direction of our FOV without changing the image resolution. In systems that use paraboloidal mirror can not change the extent of FOV without changing the overall image resolution. Paraboloidal mirror can not exclude the central downward region to conserve pixels for better use, see Figure 16.

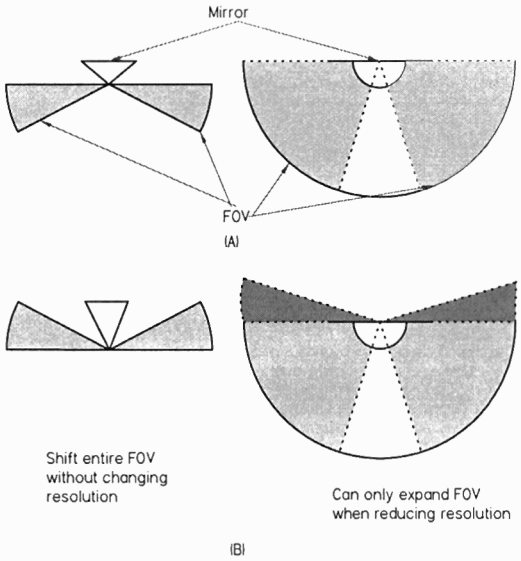

Figure 16 Cone mirror can shift the whole FOV to different angle while preserving image resolution. Parabolic mirror can only expand FOV with the result of losing resolution.

7. Conclusion

We have described a novel omni-directional stereo system that captures 3D depth and single viewpoint omni-directional view information at the same time. This new system uses only simple off-the-shelf components and achieves better resolution/data flow/price/speed tradeoff in many applications than existing omni-stereo systems.

8. Acknowledgements

This work has been supported in part by NSF-IIS-0083209, ARO/MURI-DAAH04-96-1-0007, NSF-CDS-97-03220, DARPA-ITO-DABT63-99-1-0017, and Advanced Network and Services. Special thanks to members of MOOSE Project: V. J. Kumar, Kostas Daniilidis, Elli Angelopoulou, Oleg Naroditsky, and Geoffrey Egnal for their invaluable comments and support. Also grateful thanks to members of GRASP Lab for their wonderful feedback and help.

References

1 Baker, S. and Nayar, S. K., "A Theory of Single-Viewpoint Catadioptric Image Formation," *International Journal of Computer Vision*, vol. 35, no. 2, pp. 175-196, Nov.1999.

2 Benosman, R., Maniere, T., and Devars, J. Multidirectional stereovision sensor, calibration and scene reconstruction. 1996. Proceedings of the International Conference on Pattern Recognition.
Ref Type: Conference Proceeding

3 Bogner, S. Introduction to panoramic imaging. 3100-3106. 1995. Proceedings of the IEEE SMC Conference. 1995.
Ref Type: Conference Proceeding

4 Gluckman, J. and Nayar, S. K. Rectified Catadioptric Stereo Sensors . 2000. Hilton Head Island, SC, USA, IEEE Computer Society Press. Proceedings of IEEE Conference on Computer Vision and Pattern Recognition. 2000.
Ref Type: Conference Proceeding

5 Gluckman, J. M., Thoresz, K., and Nayar, S. K. Real time panoramic stereo. 1998. Proceedings of Image Understanding Workshop. 1998.
Ref Type: Conference Proceeding

6 Hecht, E., *Optics*, 3 ed. Reading, MA, USA: Addison Wesley Longman, Inc., 1998, pp. 1-694.

7 Ishiguro, H., Yamamoto, M., and Tsuji, S. Omni-directional stereo for making global map. 540-547. 1990. Osaka, Japan, IEEE Computer Society Press. Proceedings of the 3rd International Conference on Computer Vision. 1990.
Ref Type: Conference Proceeding

8 Ishiguro, H., Yamamoto, M., and Tsuji, S., "Omnidirectional stereo," *IEEE Transactions on Pattern Analysis and Machine Intelligence*, vol. 14, no. 2, pp. 257-262, Feb.1992.

9 Kang, S. B. and Szeliski, R., "3-d scene data recovery using omnidirectional multibaseline stereo," *International Journal of Computer Vision*, vol. 25, no. 2, Nov.1997.

10 Kawanishi, T., Yamazawa, K., Iwasa, H., Takemura, H., and Yokoya, N. Generation of high resolution stereo panoramic images by omnidirectional imaging sensor using hexagonal pyramidal mirrors. 485-489. 1998. Proceedings of the International Conference on Pattern Recognition. 1998.
Ref Type: Conference Proceeding

11 Krishnan, A. and Ahuja, N., "Range estimation from focus using a non-frontal imaging camera," *International Journal of Computer Vision*, vol. 20, no. 3, pp. 169-185, 1996.

12 Lin, S. S. and Bajcsy, R. The True Single View Point (SVP) Configuration for Omni-Directional View Catadioptric System Using Cone Mirror. MS-CIS-00-24, 1-11. 2001. Philadelphia, PA, USA, Computer and Information Science

Department, University of Pennsylvania.
Ref Type: Report

13 Murray, D. W., "Recovering range using virtual multicamera stereo," *Computer Vision and Image Understanding*, vol. 61, no. 2, pp. 285-291, 1995.

14 Nayar, S. K. Sphereo: recovering depth using a single camera and two specular spheres. 1988. Proceedings of SPIE: Optics, Illumination, and Image Sensing for Machine Vision II. 1988.
Ref Type: Conference Proceeding

15 Nene, S. and Nayar, S. K. Stereo with mirrors. 1998. Bombay, India. Proceedings of IEEE International Conference on Computer Vision. 1998.
Ref Type: Conference Proceeding

16 Sarachik, K. B. Characterising an indoor environment with a mobile robot and uncalibrated stereo. 2, 984-989. 1989. Proceedings of IEEE International Conference on Robotics and Automation. 1989.
Ref Type: Conference Proceeding

17 Southwell, D., Basu, A., Fiala, M., and Reyda, J. Panoramic stereo. 1996. IEEE Computer Society Press. Proceedings of the International Conference on Pattern Recognition. 8-25-1996.
Ref Type: Conference Proceeding